

Figure 2. Fourier transforms of the rubidium K-edge transmission EXAFS for $\text{Rb}^+(18\text{C}6)\cdot\text{SCN}^-$ (—), $\text{Rb}^+(18\text{C}6)\cdot\text{Rb}^-$ (···), $\text{Rb}^+(18\text{C}6)\cdot\text{e}^-$ (---).

of such states,^{14,15} shows remarkable differences. The X-ray absorption spectrum of the rubidide $\text{Cs}^+(18\text{C}6)_2\cdot\text{Rb}^-$ (curve b) is very similar to that of Kr gas¹⁵ (curve a). The white line is virtually absent because of the low density of vacant bound excited states. Also, there is no discernible EXAFS, a result of the very large size of Rb^- (estimated radius 3.4 Å;¹⁶ nearest-neighbor distance ~ 5.5 Å). By contrast, $\text{Rb}^+18\text{C}6\cdot\text{Br}^- \cdot 2\text{H}_2\text{O}$ (curve c) shows a large white line and distinctive^{17,18} EXAFS, characteristic of Rb^+ .

The area A of the white line, normalized to unit edge jump, for all compounds studied, is given in Table I. On the one hand, the complexed rubidiums such as $\text{Rb}^+(18\text{C}6)\cdot\text{Br}^- \cdot 2\text{H}_2\text{O}$, $\text{Rb}^+(18\text{C}6)\cdot\text{SCN}^-$, $\text{Rb}^+(18\text{C}6)\cdot\text{Na}^+$, and $\text{Rb}^+(15\text{C}5)_2\cdot\text{Na}^+$ have the largest white lines with areas ranging from 20 to 30, very close to the range of 26 to 34 observed for the oxidized complexes. On the other hand, the rubidides $\text{Cs}^+(18\text{C}6)_2\cdot\text{Rb}^-$ and $\text{K}^+\text{C}222\cdot\text{Rb}^-$ have the smallest areas ($A = 1$ and 3, respectively). When both are present, e.g., $\text{Rb}^+(18\text{C}6)\cdot\text{Rb}^-$ and $\text{Rb}^+(15\text{C}5)_2\cdot\text{Rb}^-$, $A = 12$ and 18, respectively, roughly half the A values observed for the complexed rubidium systems, consistent with the fact that half of the rubidiums exist as Rb^+ . Finally, there are systems that are apparently mixtures. For example, $\text{RbK}(18\text{C}6)$, with an A value of 10 may be a mixture of $\text{Rb}^+(18\text{C}6)\cdot\text{K}^-$ and $\text{K}^+(18\text{C}6)\cdot\text{Rb}^-$ and $\text{RbK}(15\text{C}5)_2$ with $A = 16$ is probably a mixture of $\text{Rb}^+(15\text{C}5)_2\cdot\text{K}^-$ and $\text{K}^+(15\text{C}5)_2\cdot\text{Rb}^-$.

The spread of A values from 20 to 30 for complexed Rb^+ may be due to donation of electron density from the anion. Thus, the "protected" Rb^+ in $\text{Rb}^+(15\text{C}5)_2\cdot\text{Na}^+$ has $A = 29$ while for $\text{Rb}^+18\text{C}6\cdot\text{Na}^+$ $A = 19$. Also, within the 18C6 series, A decreases with decreasing ionization potential of the anions, $\text{SCN}^- \gtrsim \text{Br}^- > \text{Na}^- > \text{e}^-$.

Fourier transformed (FT) EXAFS¹⁷ for alkaliides with the $\text{Rb}^+(18\text{C}6)$ moiety are similar to those of the model compounds as illustrated in Figure 2 for $\text{Rb}^+(18\text{C}6)\cdot\text{SCN}^-$ (a), $\text{Rb}^+(18\text{C}6)\cdot\text{Rb}^-$ (b), and $\text{Rb}^+(18\text{C}6)\cdot\text{e}^-$ (c). In the former, Rb^+ is coordinated to six crown ether oxygens ($\text{Rb}-\text{O}$, 2.93–3.15 Å)⁹ and to two thiocyanate anions [$\text{Rb}-\text{N}(\text{S})$, 3.23 and 3.31 Å]. The FT shows a broad peak (phase-shift corrected) at 2.95 Å (Rb^+-O) that extends to 3.4 Å, thus masking the $\text{Rb}^+-\text{thiocyanate}$ peaks. A second peak at 3.95 Å corresponds to the $\text{Rb}^+ \cdots \text{C}$ distances. The FT for the rubidide, $\text{Rb}^+(18\text{C}6)\cdot\text{Rb}^-$ is very similar, with main

peaks at 2.95 Å (Rb^+-O) and 3.80 Å ($\text{Rb}^+ \cdots \text{C}$). The attenuation in the FT peaks from $\text{Rb}^+(18\text{C}6)\cdot\text{SCN}^-$ (a) to $\text{Rb}^+(18\text{C}6)\cdot\text{Rb}^-$ (b) results from dilution of the Rb^+ concentration (from 100% to 50%) and the absence of Rb^- EXAFS. The EXAFS of the other systems containing mixtures are also consistent with the presence of Rb^+ and Rb^- . The FT of the electride,¹⁹ $\text{Rb}^+(18\text{C}6)\cdot\text{e}^-$, in addition to the $\text{Rb}-\text{O}$ (2.7 Å) and $\text{Rb} \cdots \text{C}$ (3.8 Å) distances, has a peak at 3.4 Å which is tentatively assigned to $\text{Rb} \cdots \text{O}(\text{C})$ distances. The presence of this new peak, and the shifts of the $\text{Rb}-\text{O}$ and $\text{Rb} \cdots \text{C}$ peaks to lower distances, indicates a significant change in the local structure around Rb^+ .

In summary, the XANES and EXAFS results are fully consistent and can be used to differentiate between Rb^+ and Rb^- , thus providing new insights into the nature of alkaliides and electrides.

Acknowledgment. This work was supported by NSF Grant DMR-79-21979. CHESS is supported by NSF Grant DMR 81-12811. We thank R. Huang, M. Faber, and S. Dawes for assistance in collecting data and Z. Li, A. Ellaboudy, and M. Tinkham for providing some of the samples.

(19) This salt could be the rubidide $\text{Rb}^+(18\text{C}6)_2\cdot\text{Rb}^-$.

Reductive Homologation of CO to a Ketene-carboxylate by a Low-Valent Organolanthanide Complex: Synthesis and X-ray Crystal Structure of $[(\text{C}_5\text{Me}_5)_4\text{Sm}_2(\text{O}_2\text{CCCO})(\text{THF})_2]_2^1$

William J. Evans,*^{2a,b} Jay W. Grate,^{2b} Laura A. Hughes,^{2b} Hongming Zhang,^{2c} and Jerry L. Atwood*^{2c}

Departments of Chemistry
The University of California, Irvine
Irvine, California 92717
University of Alabama
University, Alabama 35486
Received December 17, 1984

As part of our general investigation of low-valent lanthanide chemistry³ we reported that the divalent complex $(\text{C}_5\text{Me}_5)_2\text{Sm}(\text{THF})_2$ (I) reacts with CO at atmospheric pressure.⁴ The reaction was complex and separation of the many products formed has proven difficult. Multiple products are also formed when I reacts with CO at 90 psi, but under the proper conditions one product separates in crystalline form. We report here the structure of this remarkable product and discuss its implications in the areas of CO reduction⁵ and low-valent lanthanide chemistry.

Reaction of CO at 90 psi with $(\text{C}_5\text{Me}_5)_2\text{Sm}(\text{THF})_2$ (162 mg, 0.29 mmol) in 5 mL of THF in a 3-oz Fischer-Porter aerosol

(1) Presented in part at the Third China-Japan-U.S. Symposium on Organometallic Chemistry and Catalysis, August 5-9, 1984, Santa Cruz, CA.

(2) (a) Alfred P. Sloan Research Fellow. (b) University of California, Irvine. (c) University of Alabama.

(3) (a) Evans, W. J. *J. Organomet. Chem.* **1983**, *250*, 217-226 and references therein. (b) Evans, W. J.; Hughes, L. A.; Hanusa, T. P. *J. Am. Chem. Soc.* **1984**, *106*, 4270-4272. (c) Evans, W. J.; Bloom, I.; Engerer, S. C. *J. Catal.* **1983**, *84*, 468-476. (d) Evans, W. J. In "The Rare Earths in Modern Science and Technology"; McCarthy, G. J., Rhyne, J. J., Silber, H. E., Eds.; Plenum Press: New York, 1982, Vol. 3, pp 61-70.

(4) Evans, W. J.; Bloom, I.; Hunter, W. E.; Atwood, J. L. *J. Am. Chem. Soc.* **1981**, *103*, 6507-6508.

(5) (a) Storch, H. H.; Golumbic, N.; Anderson, R. B. "The Fischer-Tropsch Reaction and Related Syntheses"; Wiley: New York, 1951. (b) Ponec, V. *Catal. Rev.-Sci. Eng.* **1978**, *18*, 1515-171. (c) Masters, C. *Adv. Organomet. Chem.* **1979**, *17*, 61-103. (d) Kung, H. H. *Catal. Rev.-Sci. Eng.* **1980**, *22*, 235-259. (e) Klier, K. *Adv. Catal.* **1982**, *31*, 243-313. (f) Dombek, B. D. *Adv. Catal.* **1983**, *32*, 325-416. (g) Muettterties, E. L.; Stein, J. *Chem. Rev.* **1979**, *79*, 479-490. (h) Bercaw, J. E.; Wolczanski, P. T. *Acc. Chem. Res.* **1980**, *13*, 121-127. Barger, P. T.; Santasiero, B. D.; Armantrout, J.; Bercaw, J. E. *J. Am. Chem. Soc.* **1984**, *106*, 5178-5186 and references therein. (i) Erker, G. *Acc. Chem. Res.* **1984**, *17*, 103-109.

(15) Stern, E. A.; Heald, S. M. In "Handbook on Synchrotron Radiation"; Koch, E. E., Ed.; North-Holland Publishing Co.: Amsterdam 1983; Vol. 1, pp 955-1014.

(16) Dye, J. L. *Angew. Chem.* **1979**, *18*, 587-598.

(17) For details of the data analysis see: (a) Teo, B. K.; Shulman, R. G.; Brown, G. R.; Meixner, A. E. *J. Am. Chem. Soc.* **1979**, *101*, 5624-5631. (b) Teo, B. K. *Acc. Chem. Res.* **1980**, *13*, 412-419. (c) Lee, P. A.; Citrin, P. H.; Eisenberger, P.; Kincaid, B. M. *Rev. Mod. Phys.* **1981**, *53*, 769-806.

(18) The high Debye-Waller factors (ca. 0.14-0.17) and hence weak EXAFS signals are consistent with large static disorder and weak ionic bonds.

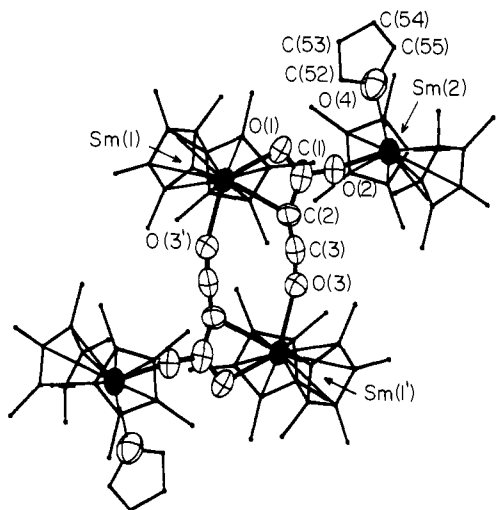


Figure 1. ORTEP plot of the molecular structure of $[(C_5Me_5)_4Sm_2(O_2CCCO)(THF)_2]$. Sm atoms are shown as darkened ellipsoids. C_5Me_5 and C_4H_8O carbon atoms are shown as dots for clarity.

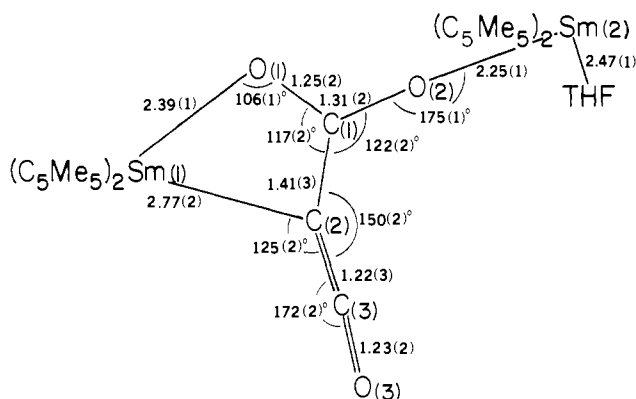


Figure 2. Bond distances (Å) and angles for one of the monomeric units of $[(C_5Me_5)_4Sm_2(O_2CCCO)(THF)_2]$.

reaction vessel ($\sim 85 \text{ cm}^3$) changes the red-purple color of I to dark brown over a 3-day period. Orange-brown crystals suitable for X-ray diffraction⁶ are formed under these conditions and have been identified as $[(C_5Me_5)_4Sm_2(O_2CCCO)(THF)_2]$ (II) (30 mg, 20%). An ORTEP plot of complex II is shown in Figure 1, and a schematic diagram with important bond distances and angles is presented in Figure 2.⁷

The structure contains an O_2CCCO moiety with bond lengths and angles consistent with a dimetal-substituted ketenecarboxylic acid. The $C(3)-O(3)$ and $C(2)-C(3)$ distances are comparable to those in other metal-substituted ketene complexes,^{8,9} and the $C(2)-C(3)-O(3)$ angle is $172(2)^\circ$. $Sm(2)$ interacts with the

O_2CCCO ligand via a $2.25(1) \text{ \AA}$ $Sm(2)-O(2)$ connection. This distance is short compared to oxygen samarium donor bond distances¹⁰⁻¹³ and is consistent with a single-bond interaction.¹⁴⁻¹⁶ However, the $C(1)-O(2)$ bond distance of $1.31(2) \text{ \AA}$ is shorter than normal $C-O$ single bonds.¹⁷ $Sm(1)$ is connected to the O_2CCCO moiety through $O(1)$ and $C(2)$ with $Sm(1)-O(1)$ and $Sm(1)-C(2)$ distances of $2.39(1)$ and $2.77(2) \text{ \AA}$, respectively. The $Sm(1)-O(1)$ length is closer to the $O \rightarrow Sm(III)$ donor bond range,¹⁰ e.g., $Sm(2)-O(4) = 2.47(1) \text{ \AA}$, than to a single-bond distance,¹⁴ while the $Sm-C$ length is longer than the few previously observed $C-Sm(III)$ distances.^{18,19} The dimer is held together by $O(3)-Sm(1)'$ connections of $2.38(1) \text{ \AA}$ consistent with an oxygen-to-metal donor bond.¹⁰

Complex II exhibits a strong IR absorption at 2100 cm^{-1} in the ketene region²⁰ and is too insoluble in inert solvents to give an NMR spectrum.

The ketenecarboxylate skeleton in II can be formally derived from three CO molecules by two one-electron reductions ($2Sm(II) \rightarrow 2Sm(III) + 2e$) plus the appropriate coupling. One-electron reduction of CO has been reported in the past primarily with alkali metal reducing agents.²¹ Less precedent exists in the literature for the CO coupling observed in II, since a $C=C-C$ linkage derived from CO requires cleavage of a carbon-oxygen bond in CO. Although cleavage of the CO triple bond followed by homologation is thought to occur in the heterogeneous Fischer-Tropsch systems,⁵ cleavage of CO by homogeneous systems rarely gives homologated products.²²

The results described above suggest that one-electron reduction chemistry of CO is a viable alternative to the heavily studied metal hydride approach to CO reduction and homologation.⁵ The strongly reducing soluble divalent organosamarium complexes such as $I^{23,24}$ provide some unique features in this regard. Alkali and alkaline earth metals are strong enough reducing agents to effect CO reduction,²¹ but since they carry no solubilizing coligands, neither these reagents nor their CO reduction products are generally soluble. The latter fact limits the possibility of multiple

(10) Complex, $O \rightarrow Sm$ donor bond distance(s) (Å): $(C_5Me_5)_2SmCl(THF)$,¹¹ 2.48(2), 2.44(2); $(C_5Me_5)_2SmI(THF)$,¹¹ 2.45(1); $(C_5Me_5)_2Sm(C_6H_5)(THF)$,¹² 2.511(4); $[(C_5Me_5)_2(Ph_3PO)Sm]_2(\mu-OCH=CHO)$,¹³ cis isomer 2.39(1), trans isomer 2.36(1), 2.39(1).

(11) Evans, W. J.; Grate, J. W.; Levan, K. R.; Doedens, R. J.; Hunter, W. E.; Zhang, H.; Atwood, J. L., in preparation.

(12) Evans, W. J.; Bloom, I.; Hunter, W. E.; Atwood, J. L. *Organometallics* **1985**, *4*, 112-118.

(13) Evans, W. J.; Grate, J. W.; Doedens, R. J. *J. Am. Chem. Soc.* **1985**, *107*, 1671-1679.

(14) Complex, $Sm-O$ distance (Å): $[(C_5Me_5)_2Sm]_2(\mu-O)$,¹⁵ 2.094(1); $(C_5Me_5)_2SmOC_6Me_4H$,¹⁶ 2.13(1); $[(C_5Me_5)_2(Ph_3PO)Sm]_2(\mu-OCH=CHO)$,¹³ cis isomer 2.147(10), 2.179(10), trans isomer 2.122(8), 2.107(7). Large $Sm-O-C$ angles as found in II are also observed in the above examples.^{15,16}

(15) Evans, W. J.; Grate, J. W.; Bloom, I.; Hunter, W. E.; Atwood, J. L. *J. Am. Chem. Soc.* **1985**, *107*, 405-409.

(16) Evans, W. J.; Hanusa, T. P.; Levan, K. R. *Inorg. Chim. Acta*, in press.

(17) $C-O$ single bond distances vary from $1.36(1) \text{ \AA}$ for $Ar-OH$ and acid and ester $RCO-OR'$ to $1.43(10) \text{ \AA}$ for aliphatic alcohols and ethers: *Spec. Publ. Chem. Soc.* **1965**, *18*, M665. Allen, F. H.; Kirby, A. J. *J. Am. Chem. Soc.* **1984**, *106*, 6197-6200 and references therein.

(18) Complex, $Sm-C$ distance (Å): $(C_5Me_5)_2Sm(C_6H_5)(THF)$,¹² 2.511(8); $[(CH_2C_5H_4)_2Sm(\mu-C \equiv CCMe_3)]_2$,¹⁹ 2.55(1).

(19) Evans, W. J.; Bloom, I.; Hunter, W. E.; Atwood, J. L. *Organometallics* **1983**, *2*, 709-714.

(20) IR of crystalline sample whose identity as II was confirmed by determining the unit cell parameters of two crystals in the sample (KBr, cm^{-1}): 2900 (vs, br), 2100 (vs), 1530 (w), 1480 (vs), 1450 (vs), 1370 (m), 1250 (vs), 1170 (m), 1070 (m), 1010 (s), 865 (s), 760 (m).

(21) (a) Liebig, *J. Ann.* **1834**, *11*, 182. (b) Joannis, A. C. *R. Hebd. Seances Acad. Sci.* **1893**, *116*, 1518; **1914**, *158*, 874-876. (c) Orchin, M.; Wender, I. *Catalysis* **1957**, *5*, Chapter 1 and references therein. (d) Büchner, W. *Helv. Chim. Acta* **1963**, *46*, 2111-2120. (e) Weiss, E.; Büchner, W. *Helv. Chim. Acta* **1963**, *46*, 1121-1127. (f) Büchner, W. *Chem. Ber.* **1966**, *99*, 1485-1492 and references therein. (g) Besson, J.; Renaud, M. *Rev. Chim. Miner.* **1969**, *6*, 157-168.

(22) Cf.: Planalp, R. P.; Andersen, R. A. *J. Am. Chem. Soc.* **1983**, *105*, 7774-7775 and references therein.

(23) The related divalent organosamarium complexes $(C_5Me_5)_2Sm^{3b}$ and $[(C_5Me_5)_2Sm(\mu-I)(THF)]_2$ ²⁴ are also available and do in fact react with CO.

(24) Evans, W. J.; Grate, J. W.; Bloom, I.; Choi, H. W.; Hunter, W. E.; Atwood, J. L. *J. Am. Chem. Soc.* **1985**, *107*, 941-946.

(6) The space group is $P1$ with $a = 13.047(4) \text{ \AA}$, $b = 13.564(6) \text{ \AA}$, $c = 16.028(5) \text{ \AA}$, $\alpha = 78.51(5)^\circ$, $\beta = 70.60(4)^\circ$, $\gamma = 68.63(6)^\circ$, $U = 2481.6 \text{ \AA}^3$, and $D_c = 1.33$ for $Z = 1$ (tetrameric unit). Least-squares refinement on the basis of 3297 observed reflections led to a final $R = \sum(|F_o| - |F_c|) / \sum |F_o| = 0.068$. Hydrogen atoms were not included, and the ring carbon atoms were refined with isotropic temperature factors. The thermal motion of all other atoms was dealt with anisotropically.

(7) Full crystallographic data are given as supplementary material.

(8) $(C_5H_5)(CO)(PMe_3)_2W-C(C_6H_4Me)=C=O$ has $C=C = 1.24(3) \text{ \AA}$, $C=O = 1.21(3) \text{ \AA}$: Kreissl, F. R.; Frank, A.; Schubert, U.; Lindner, L. L.; Huttner, G. *Angew. Chem., Int. Ed. Engl.* **1976**, *15*, 632-633.

(9) Bent η^2 -ketene complexes generally have longer $C=C$ and $C=O$ distances: Redhouse, A. D.; Hermann, W. A. *Angew. Chem., Int. Ed. Engl.* **1976**, *15*, 615-616. Hermann, W. A.; Plank, J.; Ziegler, M. L.; Weidenhammer, K. *J. Am. Chem. Soc.* **1979**, *101*, 3133-3135. Fachinetti, G.; Biran, C.; Floriani, C.; Chiesa-Villa, A.; Guastini, C. *Inorg. Chem.* **1978**, *17*, 2995-3002. Gambarotta, S.; Pasquali, M.; Floriani, C.; Chiesa-Villa, A.; Guastini, C. *Inorg. Chem.* **1981**, *20*, 1173-1178. Bristow, G. W.; Hitchcock, P. B.; Lappert, M. F. *J. Chem. Soc., Chem. Commun.* **1982**, 462-464. Moore, E. J.; Straus, D. A.; Armantrout, J.; Santasiero, B. D.; Grubbs, R. H.; Bercaw, J. E. *J. Am. Chem. Soc.* **1983**, *105*, 2068-2070.

CO homologation. Soluble, strongly reducing, low-valent, transition-metal complexes are available, but with CO they form carbonyl complexes.²⁵ Hence, the low affinity of lanthanide ions to form stable CO complexes, the high oxophilicity of the lanthanides, and the strongly reducing Sm(II) → Sm(III) couple in soluble complexes allow distinctive CO chemistry to occur with organosamarium reagents. Further studies on these and related systems are in progress.

Acknowledgment. We thank the National Science Foundation for support of this research and the Alfred P. Sloan Foundation for a Research Fellowship (to W.J.E.).

Registry No. I, 79372-14-8; II, 96348-41-3; CO, 630-08-0.

Supplementary Material Available: Tables of crystal data, bond distances, angles, final fractional coordinates, thermal parameters, and observed and calculated structure factor amplitudes plus a fully numbered ORTEP plot (26 pages). Ordering information is given on any current masthead page.

(25) Titanocene chemistry provides one example: Bercaw, J. E.; Marvich, R. H.; Bell, L. G.; Brintzinger, H. H. *J. Am. Chem. Soc.* **1972**, *94*, 1219-1238. Bottrill, M.; Gavens, P. D.; McMeeking, J. In "Comprehensive Organometallic Chemistry"; Wilkinson, G. W., Stone, F. G. A., Abel, E. W., Eds., Pergamon Press: Oxford, 1982; Chapter 22.2.

Carboxylate Bridge Exchange Reactions in the $[\text{Fe}_2\text{O}(\text{O}_2\text{CR})_2]^{2+}$ Core. Synthesis, Structure, and Properties of Phosphodiester-Bridged Complexes

William H. Armstrong and Stephen J. Lippard*

Department of Chemistry
Massachusetts Institute of Technology
Cambridge, Massachusetts 02139

Received January 14, 1985

The recently reported binuclear iron(III) complexes containing the $[\text{Fe}_2\text{O}(\text{O}_2\text{CR})_2]^{2+}$ core^{1,2} are currently the best available structural and spectroscopic models for the spin-coupled diiron(III) centers in hemerythrin³ and ribonucleotide reductase.⁴ Reactivity studies of this core structure have been initiated.^{1b,5,6} In the hydrotris(1-pyrazolyl)borate derivative, $[(\text{HB}(\text{pz})_3)\text{FeO}(\text{O}_2\text{CCH}_3)_2\text{Fe}(\text{HB}(\text{pz})_3)]$ (**1**), facile ¹⁸O-exchange^{1b} and protonation⁵ reactions of the bridging oxygen atom have been observed. The fact that protonation of the oxo bridge is accompanied by expansion of the core suggested to us that concomitant exchange reactions of the bridging carboxylate groups might be feasible. Here we describe the results of initial investigations of carboxylate bridge exchange reactions with carboxylic and diesterified phosphoric acids. Interaction of the μ -oxodiiron(III) center with phosphate esters is of interest since iron(III) phosphate interactions occur in ferritin,⁷ phosvitin,⁸ and Fe^{III} -ATP model complexes⁹ and are possibly involved in the phosphate-containing form of uteroferrin¹⁰ and the binding of nucleoside diphosphate substrates

(1) (a) Armstrong, W. H.; Lippard, S. J. *J. Am. Chem. Soc.* **1983**, *105*, 4837-4838. (b) Armstrong, W. H.; Spool, A.; Papaefthymiou, G. C.; Frankel, R. B.; Lippard, S. J. *Ibid.* **1984**, *106*, 3653-3667. (c) Spool, A.; Williams, I. D.; Lippard, S. J. *Inorg. Chem.*, in press.

(2) Wieghardt, K.; Pohl, K.; Gebert, W. *Angew. Chem., Int. Ed. Engl.* **1983**, *22*, 727.

(3) (a) Stenkamp, R. E.; Sieker, L. C.; Jensen, L. H. *J. Am. Chem. Soc.* **1984**, *106*, 618-622. (b) Klotz, I. M.; Kurtz, D. M., Jr. *Acc. Chem. Res.* **1984**, *17*, 16-22. (c) Wilkins, R. G.; Harrington, P. C. *Adv. Inorg. Biochem.* **1983**, *5*, 51-85. (d) Sanders-Loehr, J.; Loehr, T. M. *Ibid.* **1979**, *1*, 235-252.

(4) (a) Reichard, P.; Ehrenberg, A. *Science (Washington, D.C.)* **1983**, *221*, 514-519. (b) Sjöberg, B.-M.; Graslund, A. *Adv. Inorg. Biochem.* **1983**, *5*, 87-110. (c) Lammers, M.; Follman, H. *Struct. Bonding (Berlin)* **1983**, *54*, 27-91.

(5) Armstrong, W. H.; Lippard, S. J. *J. Am. Chem. Soc.* **1984**, *106*, 4632-4633.

(6) Wieghardt, K.; Pohl, K.; Ventur, D. *Angew. Chem.*, in press.

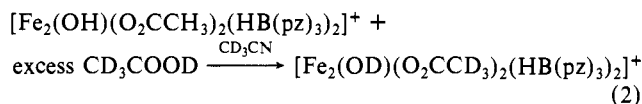
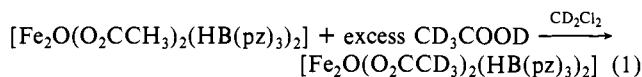
(7) Theil, E. C. *Adv. Inorg. Biochem.* **1983**, *5*, 1-38.

(8) Taborsky, G. *Adv. Inorg. Biochem.* **1983**, *5*, 235-279.

(9) Mansour, A. N.; Thompson, C.; Theil, E. C.; Chasteen, N. D.; Sayers, D. E. *J. Biol. Chem.*, in press.

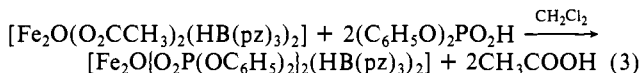
to ribonucleotide reductase. Moreover, we are concerned with the iron-promoted hydrolysis of phosphate esters¹¹ which may be of relevance to the phosphatase activity displayed by the purple acid phosphatases and uteroferrin.¹⁰

In both **1**¹ and its protonated derivative, $[(\text{HB}(\text{pz})_3)\text{Fe}(\text{OH})(\text{O}_2\text{CCH}_3)_2\text{Fe}(\text{HB}(\text{pz})_3)](\text{ClO}_4)$ (**2**),⁵ the bridging acetate groups exchange readily with perdeuterioacetic acid in solution as revealed by proton NMR spectroscopy (Figure 1). These reactions (eq 1 and 2) were carried out at room temperature with addition of 10 and 12.5 equiv of CD_3COOD for **1** and **2**, respectively. ¹H NMR spectra of the reactions, recorded ~ 0.5



h after mixing, reveal that the bridged diiron(III) structures remain intact and that resonances associated with CH_3 of the coordinated acetate groups vanish as the perdeuterioacetate analogues are formed.

By making use of a related reaction (eq 3) we have prepared the diphenylphosphate-bridged complex, $[\text{Fe}_2\text{O}(\text{O}_2\text{P}(\text{OC}_6\text{H}_5)_2)_2(\text{HB}(\text{pz})_3)_2]$ (**3**). To a solution of 1.002 g (1.491 mmol) of **1** in



500 mL of CH_2Cl_2 was added a solution of 0.742 g (2.98 mmol) of $(\text{C}_6\text{H}_5\text{O})_2\text{PO}_2\text{H}$ in 50 mL of CH_2Cl_2 dropwise over approximately 5 min. The brown-green color of **1** in solution quickly changed to emerald-green. The reaction mixture was stirred for 1 h and then the solvent was stripped off with a rotary evaporator to yield a dark green oil. This oil was dissolved in 30 mL of CCl_4 , and the resulting solution was allowed to stand for 3 days at ambient temperature during which time a microcrystalline green precipitate formed. The solid was filtered, washed with 10 mL of CCl_4 and then 2×10 mL portions of hexanes, powdered, and dried under vacuum to afford 1.394 g (75.6%) of the CCl_4 solvate of **3**. A similar procedure was used to prepare $[\text{Fe}_2\text{O}(\text{O}_2\text{P}(\text{OC}_2\text{H}_5)_2)_2(\text{HB}(\text{pz})_3)_2]$. Further purification of **3** was achieved by recrystallization from CHCl_3 with hexanes layered on top. Crystals of $3 \cdot \text{CHCl}_3$ suitable for X-ray diffraction studies¹² and elemental analysis¹³ were obtained by this method.

The structure of **3** (Figure 2) reveals that the oxo-bridged diiron(III) core is retained upon exchange of carboxylate for diphenylphosphate ligands. Two bidentate diphenylphosphate bridges now span the μ -oxodiiron(III) core, and the resulting $[\text{Fe}_2\text{O}(\text{O}_2\text{P}(\text{OPh})_2)_2]^{2+}$ unit is capped by hydrotris(1-pyrazolyl)borate ligands. The $\text{Fe}-\text{O}_{\text{oxo}}$ distances are slightly longer in **3** than in **1**, 1.808 (4) vs. 1.784 (4) Å, respectively. The larger $\text{Fe}-\text{O}-\text{Fe}$ angles, 134.7 (3)° vs. 123.6 (1)°, and resulting greater $\text{Fe} \cdots \text{Fe}$ separation, 3.337 (1) vs. 3.146 (1) Å, in **3** are presumably due to the increased $\text{O} \cdots \text{O}$ separation in phosphate compared to carboxylate ligands. The $\text{Fe}-\text{N}$ and $\text{Fe}-\text{O}_{\text{phosphate}}$ bond distances are typical for high-spin iron(III), and lengthening of $\text{Fe}-\text{N}$ distances trans to the bridging oxo atoms for **3** is a feature also

(10) Antanaitis, B. C.; Aisen, P. *Adv. Inorg. Biochem.* **1983**, *5*, 111-136.

(11) For related work see: Jones, D. R.; Lindoy, L. F.; Sargeson, A. M. *J. Am. Chem. Soc.* **1984**, *106*, 7807-7819 and references cited therein.

(12) X-ray analysis: The compound $[\text{Fe}_2\text{O}(\text{O}_2\text{P}(\text{OC}_6\text{H}_5)_2)_2(\text{HB}(\text{pz})_3)_2] \cdot \text{CHCl}_3$ crystallizes in the monoclinic system, space group $P2_1/n$, with $a = 11.940$ (2) Å, $b = 20.105$ (4) Å, $c = 22.155$ (3) Å, $\beta = 96.56$ (1)°, $V = 5283.6$ Å³, $\rho_{\text{obsd}} = 1.48$ (1) g cm⁻³, $\rho_{\text{calcd}} = 1.473$ g cm⁻³, $Z = 4$. With the use of 4693 unique reflections ($F_o > 6\sigma(F_o)$) collected at ca. 296 K with $\text{Mo K}\alpha$ ($\lambda = 0.7107$ Å) radiation out to $2\theta = 46^\circ$ on a single crystal X-ray diffractometer, the structure was solved by standard direct and difference Fourier methods and refined by using 540 variables to a current value of the discrepancy index R_1 of 0.059. Atomic positional and thermal parameters are provided as supplementary material. Full details will be reported elsewhere.

(13) Elemental analysis: Calcd for $\text{Fe}_2\text{C}_{43}\text{H}_{41}\text{B}_2\text{Cl}_3\text{N}_{12}\text{O}_9\text{P}_2 \cdot (3 \cdot \text{CHCl}_3)$: Fe, 9.53; C, 44.09; H, 3.53; Cl, 9.08; N, 14.35; P, 5.29. Found: Fe, 9.28; C, 43.72; H, 3.50; Cl, 9.09; N, 14.44; P, 5.06.